3D LOCALIZATION OF EEG ELECTRODE POSITIONS AND REGISTRATION WITH HEAD SURFACE MRI DATA

G. Grabner*, A. Janke**, G. Galloway** and Ch. Kargel*

* Division of MedIT, Carinthia Tech Institute, University of Applied Sciences, Klagenfurt, Austria
** Centre for Magnetic Resonance, University of Queensland, Brisbane, Australia

ggrabner@gmx.at, c.kargel@cti.ac.at

Abstract: The evaluation and tracking of cortical function via scalp-recorded quantitative electroencephalograms (qEEG) and concurrent source localization is a promising field for acute patient management and therapeutical monitoring of e.g. stroke and head-injury. This requires accurate registration of EEG electrode positions with pre-existing structural scans that reveal a subject's individual anatomy. This paper focuses on the localization of EEG electrodes in three-dimensional (3D) space and their registration with magnetic resonance imaging (MRI) volume data. The performance of several different surface-based registration algorithms is evaluated - in terms of registration error and processing time - on experimental data. Furthermore, registration performance is investigated as a function of data decimation.

Introduction

The correlation of anatomy and function is one of the most important tasks in modern brain imaging techniques. Electroencephalogram (EEG) (and also magnetoEG) methods have a number of important advantages over all other functional imaging modalities currently used to understand the functional organization of the human brain. These methods provide a very high temporal resolution, only restricted by the rate at which the signals are sampled, and they are non-invasive, widely available and relatively cheap. However, EEG has a fundamental source identification problem known as the so-called inverse problem, i.e. the identification of the distribution of sources inside the brain that generate the voltage measured over an array of sensors distributed on the scalp surface. The main difficulty when dealing with these kind of problems is its ill-posed character due to the nonuniqueness of the solution. Put another way, there is an infinite number of generator configurations that result in the same voltage over the scalp surface. Much literature has been devoted to the solution of the inverse problem and the reader is referred to it at this point [1-5]. A quantitative electroencephalogram (qEEG), also referred to as brain electrical activity mapping (BEAM), enhances traditional surface EEGs by transforming the data from a relatively large number of surface electrodes (24+) into a topographic image. These enhanced images of brain activity are then placed on a schematic map of the brain, and the data are analyzed by the size, locality and frequency of the activity. These activity data are subsequently compared to a database of normal patient brainwave activity to determine specific seizure types, focality or possible underlying medical conditions. Applications of qEEG include the evaluation of Alzheimer's disease, cerebral vascular disease, epilepsy, dementia and encephalopathy. Tomographic qEEG has been introduced for the 3D in-vivo visualization of the sources of abnormal EEG oscillations [6]. It has also been shown to correctly identify the anatomical locus of hyper-acute, acute and chronic stroke [7].

For successful qEEG analysis it is advantageous to localize effects seen in EEG using a subject's individual anatomy as opposed to an average model of structure. The initial step within this framework is to acquire both 3D positional EEG electrode and magnetic resonance imaging (MRI) data. This paper describes how EEG electrode positions can be determined, and then focuses on the methods to register the EEG surface electrodes with respect to MRI volume data acquired from the same patient. Monitoring qEEG changes and accurate source localization due to precise registration will assist in diagnosis and subsequent treatment of patients (e.g. for evaluating the recovery of hand sensorimotor function that has been compromised by a stroke).

Materials and Methods

The task at hand is divided into three main parts: First, the determination of the EEG electrode positions in 3D and derivation of the corresponding point set. Second, the MRI volume scan and extraction of the head surface point set, and third, the 3D registration of those two point sets and assessment of the registration performance.

1. Determination of the EEG electrode positions

Electrode positions are determined by employing a tracking system (FASTRAK Polhemus, USA) which uses electro-magnetic fields to determine the 3D position of a remote object. These electro-magnetic fields are transmitted by an assembly of three concentric, stationary antennas (called the transmitter, see Figure 1). The detection of the electro-magnetic fields is based on three concentric, remote sensing antennas (called the receiver). The received signals are inputted into an algorithm that computes the receiver's position and orientation relative to the transmitter with a

ISSN: 1727-1983

positional accuracy of ±80 microns when the receivers are located within 76 cm of the transmitter [8]. As the system is electro-magnetic it is important that the operating area (≈ three times the distance from the transmitter to the furthest point to be localized) is free of metal. To determine the positions of several EEG electrodes in 3D space and their configuration with respect to one another, four receivers are needed: one for the EEG electrode positions by repeatedly using a stylus-pen, and three to correct patient (head) movements between stylus-pen acquisitions by using appropriate coordinate transformations. For this study, the additional three receivers were located on the forehead, and the left and right mastoids, respectively. An EEG cap with 64 electrodes was used (see Figure 1) which means that altogether 64x4=256 receiver position readings were necessary to determine the positions of all EEG electrodes with respect to the three reference receivers.

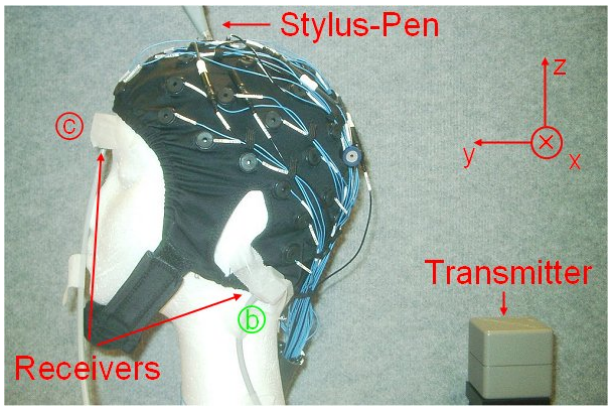

Figure 1: Setup to determine the 64 EEG electrode positions on the cap by using a stylus-pen and reference receivers.

Generally, a coordinate transformation of a point $p_A(x,y,z)$ in one Cartesian coordinate system A to $p_B(x,y,z)$ in another Cartesian coordinate system B can be defined (using vector notation):

$$\overrightarrow{p_B} = T_{B\to A}^{-1} * \overrightarrow{p_A} \qquad T_{B\to A} = (\overrightarrow{e_x}\,\overrightarrow{e_y}\,\overrightarrow{e_z}\,B_0) \quad (1)$$

where the transformation matrix $T_{B->A}$ is defined by the three unity vectors $\overrightarrow{e_x}, \overrightarrow{e_y}, \overrightarrow{e_z}$ and the origin B_0 (here at the receiver located on the forehead) of the coordinate system B [9]. The three unity vectors were derived from

$$\overrightarrow{B_z} = (\vec{a}-\vec{b})\times(\vec{a}-\vec{c}) \quad \overrightarrow{B_y} = \vec{c}-\vec{b} \quad \overrightarrow{B_x} = \overrightarrow{B_y}\times\overrightarrow{B_z} \quad (2)$$

by normalization, where $\vec{a}$ and $\vec{b}$ represent the 3D receiver positions at the right and the left mastoid, and $\vec{c}$ the receiver position at the forehead. "×" is the vector cross product. Figure 2 shows the EEG electrode positions before and after the coordinate transformations and demonstrates the successful compensation of head movements during data acquisition.

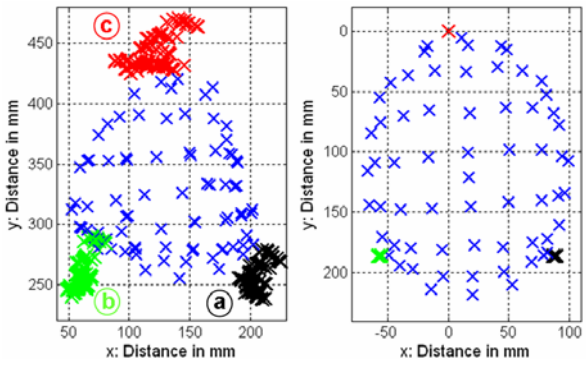

Figure 2: Left: positional raw data directly from the tracking system; right: coordinate-transformed EEG electrode positions (both top view). The black (a), green (b) and red (c) crosses represent the positions of the three additional receivers for all 64 acquisitions performed.

2. Head surface area extraction from MRI scans

It is advantageous to apply MRI scan sequences that provide high contrast in order to accurately extract the head surface (i.e. the air-skin border). T1-weighted sequences are a good choice. The 3D head surface area is found from multiple 2D slices (like the ones shown in Figure 3) of a 3D MRI data set acquired on a whole-body MRI system with a TEM head coil using a MPRAGE sequence with T_E=3 ms and T_R=2500 ms (T_E and T_R represent the echo and repetition time, respectively).

Several methods can be used for image segmentation and air-skin edge detection. For segmentation, we decided to apply a global thresholding technique, optimal in terms of classification error that generates binary images from all 2D MRI slices, followed by binary morphological closing with circular-shaped structuring elements. Morphological closing combines the dilation and erosion functions [10] and ensures proper boundary detection, even in critical areas like the nose or eyeballs (see Figure 3, right). For edge detection, first-order gradient spatial filters of the Sobel type were used in horizontal and vertical directions [11]. Figure 3 shows standard transverse MRI head slices, and overlaid in red the magnitude of the gradient which represents the air-skin border. It was not necessary to apply edge-linking procedures, which are usually very tedious.

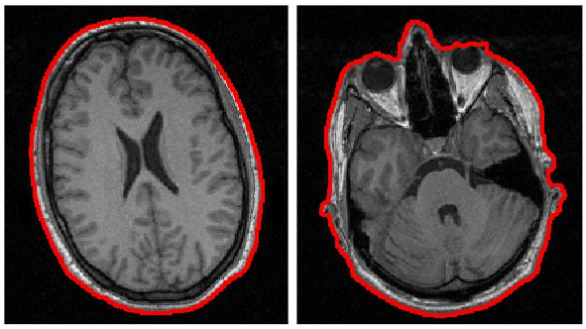

Figure 3: Gradient-based edge detection performed after image segmentation and binary closing results in the edge overlaid in red on the original images. The MRI scan was performed on a Bruker Medspec 4 Tesla whole-body MRI system providing cubic voxels with 1x1x1 mm^3.

ISSN: 1727-1983

The entire head surface area as extracted from the 3D MRI dataset is illustrated in Figure 4.

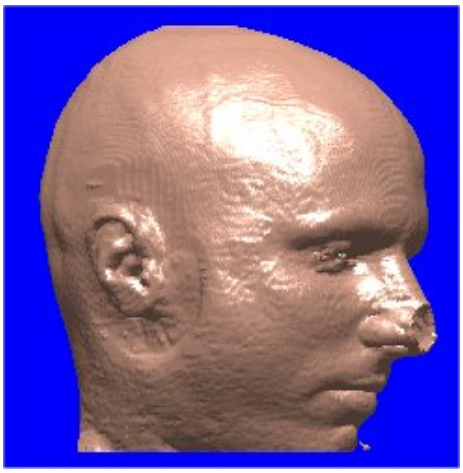

Figure 4: Entire head surface built from 255 transversal MRI slices like the ones in Figure 3. For display purposes, surface interpolation and shading were applied.

3. 3D registration of EEG electrode locations and MRI volume data

Registration is the process of aligning structures acquired with different sensors or with the same sensor at different times [12]. Medical image registration has a wide range of applications, one of which is combining functional information from e.g. PET with morphological information from e.g. CT or MRI (in our case functional information is from qEEG). This "data fusion" involves determining a transformation that relates spatial information from one modality to the other. The complexity of this transformation can be specified by the degrees of freedom (DOF) and depends on the dimensionality and constraints of the structures to be registered. Most often, and especially in this work, the assumption is very much justified that internal anatomy of the patient's head is not distorted or changed in spatial relationships so that it can be considered as a "rigid body". As a result, a transformation with only six DOF (three translations and three rotations) can be used for 3D registration. Non-rigid registration requires many more DOF, e.g. for registration of tissue that deforms over time or registration of images to those from another individual.
Registration algorithms can be divided into algorithms that use a number of either corresponding points or corresponding surfaces, or operate directly on the image intensities, the latter building upon crosscorrelation, joint probability/entropy, and mutual information [13].

The most popular registration algorithms are surface-based and minimize some measure of distance between the two surfaces to be registered. In this paper we focus on the "head and hat" and the "iterative closest point" algorithms for the registration of EEG electrode point sets with MRI surface data.

A. In the *"head and hat"* algorithm the contours of the surface extracted from the higher resolution modality represent the head while the hat is a set of unconnected 3D points that correspond to the same surface in the other modality [14]. The algorithm starts a series of trials to iteratively fit the rigid hat surface to the head. This process stops when the sum of the squares of the distances between each hat point and the head is minimized. The head and hat algorithm has been used with considerable success for registering images of the head [15].

In this paper we investigate two slightly modified versions of the traditional head and hat algorithm. The 3D registration is carried out by minimizing the function $f(\vec{t},\boldsymbol{R})$ defined in Eqns. 3 and 4 which finds the minimal average distances (=*error*) between the two surface point sets. Here, the head surface is represented by the point set extracted from digital 3D MRI data while the hat surface is represented by the coordinate-transformed (Eqns. 1 and 2) EEG electrode positions.

$$error=\min_{\vec{t},\boldsymbol{R}}\left(f_{1,2}(\vec{t},\boldsymbol{R}) \right)$$

$$SAD=f_1(\vec{t},\boldsymbol{R})=\left(\frac{1}{n}*\sum_{i=1}^{n}\left\| \overrightarrow{p_i} -(\vec{e_i}+\vec{t})*\boldsymbol{R} \right\|*w_i \right) \qquad (3)$$

$$SSD=f_2(\vec{t},\boldsymbol{R})=\sqrt{\left(\frac{1}{n}*\sum_{i=1}^{n}\left\| \overrightarrow{p_i} -(\vec{e_i}+\vec{t})*\boldsymbol{R} \right\|^2*w_i \right)} \qquad (4)$$

In the rest of the paper we refer to the measures defined in Eqn. 3 as SAD (sum of absolute distances) and to the one in Eqn. 4 as SSD (sum of squares of distances). n represents the total number of EEG electrodes and $\|$ is the operator norm. $\overrightarrow{pi}$ represents the closest point of the head surface point set to the position $\vec{e_i}$ of the i^{th} EEG electrode. $\vec{t}$ is the 3D translation vector while $\boldsymbol{R}$ is the rotation matrix as applied to the EEG electrode point set. w_i are experimentally determined weighting factors to compensate for the non-uniformly distributed electrodes on the EEG cap (higher density in the back of the cap).

The parameters $\vec{t}$ and $\boldsymbol{R}$ are changed in the minimization process to achieve the minimal registration *error*. We applied the Nelder-Mead simplex method which is a simple, iterative, multidimensional method for nonlinear unconstraint optimization [16]. This method attempts to minimize a scalar-valued nonlinear function without requiring the evaluation or existence of derivatives and thus falls into the class of direct search methods. The simplex method is fairly easy to implement and relatively robust but can be inefficient (slow) for certain problems.

B. The "*iterative closest point, ICP"* algorithm has been widely applied in surface-based medical image registration [13, 17]. Here, one surface is usually represented by a set of points while the other can be made up of e.g. triangular patches. The algorithm works in two stages and iterates. The first stage involves finding the closest point on a patch to each of the surface points. The second stage then finds a rigid-body transformation that registers the closest point set to the surface point set based on corresponding homologous landmarks in the two point sets. This process is repeated until the smallest distance between the two surfaces

ISSN: 1727-1983

is found, e.g. until the root-mean-square error drops by less than a preset value. A more detailed explanation of the ICP method can be found in [17, 18].

Pre-registration: Most registration methods including the ICP and head and hat algorithms have the same weakness, namely finding local minima of the distance measure when the surfaces exhibit rotational symmetries. This risk can be reduced by gradually increasing the spatial resolution to refine the registration accuracy, combined with outlier rejection to ignore erroneous points in order to prevent gross misregistration.

Within the framework of this paper, we decided to implement another way of reducing the likelihood of finding local minima, namely to perform pre-registration. This ensures a reasonably good match at the start of the iterative registration process so that the global minimum or at least a satisfactory local minimum (depending on the registration error accepted and the processing time available) can be reached. Thus, it is imperative to align the two surface point sets (see Figure 5) in terms of translations and rotations as precisely as possible prior to 3D registration.

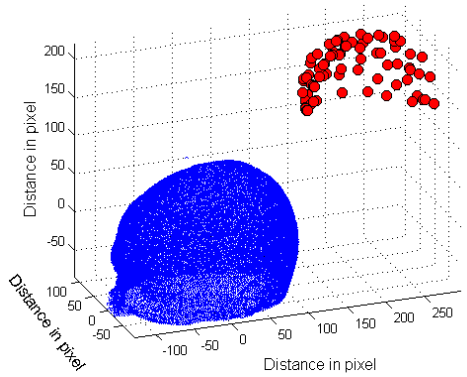

Figure 5: The raw head surface point set (blue) extracted from MRI data and the point set (red) of the 64 EEG electrodes before pre-registration. One distance unit (=pixel) equals 1 mm in all figures shown in this paper.

We greatly reduced the rigid translations between the two 3D point sets by calculating their centroids and aligning them. This was followed by a translation in *z* direction so that the top of both point sets had the same *z* coordinate. This is a fast and easy way of taking partial volume effects into account since most often the MRI point set has a larger extension in *z* direction compared with the EEG electrode point set. Higher performance - but also computationally more expensive - methods exist, e.g. [19].

The rigid body rotations in the *xy* plane were compensated for by using singular value decomposition (SVD) [20]. SVD is a common method to detect the spatial orientation of a structure. It factorizes an *M* x *N* (here real-valued) matrix **X** into the product of two orthonormal matrixes **U** and **V** of sizes *M* x *M* and *N* x *N*, respectively, and an *M* x *N* matrix **S** with non-negative singular diagonal elements:

$$\mathbf{X}=\mathbf{U}*\mathbf{S}*\mathbf{V}^{T}.$$

A geometrical interpretation of SVD is that the image of the unit sphere under any *M* x *N* matrix multiplication is a hyperellipsoid. Considering the three factors of the SVD separately in 2D, note that $\mathbf{V}^T$ is a pure rotation of the unit circle to coincide with the coordinate axes. Second, the circle is stretched by **S** in the directions of the coordinate axes to form an ellipse. The third step rotates the ellipse by **U** into its final position. The columns of **U** are denoted by the vectors $\vec{u_i}$, the principal axes of the final ellipse.

A direct consequence of the geometric interpretation is that the largest singular value of **S** measures the "magnitude" of **X**, i.e. the longest principal semi-axis of the hyperellipsoid. If a hyperellipsoid is to be approximated with a line segment, the best one can do is to take the line segment as the longest axis of the ellipsoid. If the longest and second longest axes of the ellipsoid are to be taken, one gets the best approximation by a 2D ellipse, and so on for higher dimensionalities.

The point sets in this study are represented by *M* x *3* matrices of which only the *x* and *y* components were taken to calculate two major axes using SVD. Figure 6 shows the raw MRI head surface and the EEG electrode position point sets. Overlaid are the major 2 axes in the horizontal *xy* plane. The two corresponding matrices **V** from SVD containing the spatial orientations are then used to pre-register the two 3D point sets by rotating the EEG point set, see Figure 7.

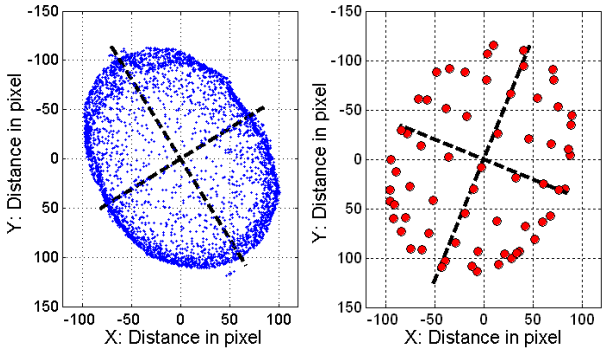

Figure 6: Top views of the MRI head surface (left) and the EEG electrode position point sets (right). The spatial orientations determined by SVD analysis are shown as black broken lines (major axes of ellipses in the *xy* plane that best approximate the point sets).

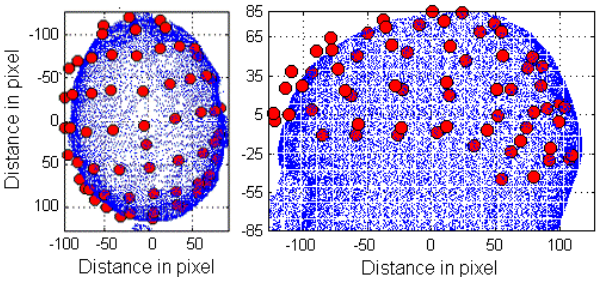

Figure 7: Both point sets after pre-registration, shown on top of each other with full visibility of all points, even for those at the backside. It can be seen that after pre-registration some misregistration remains.

ISSN: 1727-1983

Results

Upon pre-registration, the surface point sets derived from MRI and electromagnetic EEG electrode tracking were registered using the SAD, SSD and ICP algorithms described in the "Materials and Methods" section. All processing methods in this paper were implemented in MATLAB™ (The MathWorks Inc., Natick). Figure 8 representatively shows the final registration result when the SAD method was used.

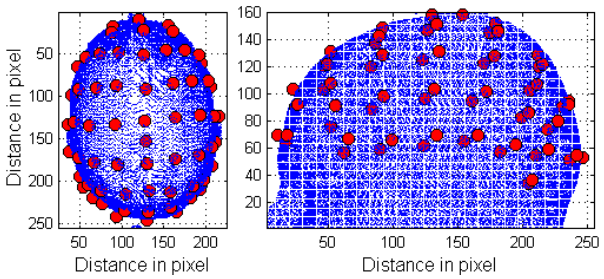

Figure 8: Registration of the 64 EEG electrode positions (red) with the MRI point set (blue) using pre-registration and the SAD method. The results with SSD and ICP were virtually identical on visual examination and thus are not shown.

The result presented in Figure 8 was derived using a head surface point set that was decimated by a factor of 10 compared with the entire head surface MRI point set containing 197,000 points. After pre-registration (see Figure 7) an average error of ≈4.95 mm per electrode existed. Registration performed with these two pre-registered point sets using the SAD, SSD and ICP methods gave almost identical average errors of approximately 2.3 mm. Thus the registration process decreased the average errors by about 50%. This percentage is strongly dependent on the performance of the applied pre-registration.

Another goal of this paper was to investigate the influences of MRI head surface data decimation (starting at a spatial resolution of 1x1x1 mm^3) on the registration time and error. First, decimation was applied only to the transverse (*xy*) MRI planes, second only in axial (*z*) direction, and third in the transverse and axial directions simultaneously following several different reduction schemes. The third option was necessary in order to achieve larger decimations factors of up to 25 and keep spatial resolution in all 3 directions approximately equal. It was found (not shown) that the method for data decimation is not critical. For the data sets used in this paper and decimation factors of up to about 15 neither the registration error nor time significantly depended on how the data were reduced. This is mostly due to the large spatial oversampling of the original MRI point set. For data decimation factors between 15 and 25 we applied the decimation scheme that provided the smallest registration errors.

A reduction of the MRI point set results in a decreased spatial resolution, no matter what the scheme for data decimation is. In order to be able to compare the registration performance of SAD, SSD, and ICP we first found the best match of the MRI and EEG electrode point sets using the different distance measures defined earlier. Upon registration, we then calculated the average linear registration error per electrode which we plotted in Figure 9. When the entire (=undecimated) head surface MRI point set was used for 3D registration the average error for the SAD method was ≈1.55 mm. As can be seen in Figure 9, all three methods exhibit approximately the same registration errors for data decimation factors of up to 25. When the methods were tested for reasons of comparison with experimental point sets derived from MRI only, the errors were at least one order of magnitude lower than those found when registering multi-modality MRI and EEG point sets. It is very difficult in practice to assure firm contact of all EEG electrodes with the head surface. This can be caused by different amounts of hair and applied electrode contact gel as well as spatially varying strain of the EEG cap. Overall, our experiments revealed that the surface points derived from the utilized tracking system and standard MRI scans can have average distances of about 1-2 mm. It is clear that even the best rigid registration method is not able to reduce the registration error below this value. However, this Figure is sufficient for successful qEEG analysis.

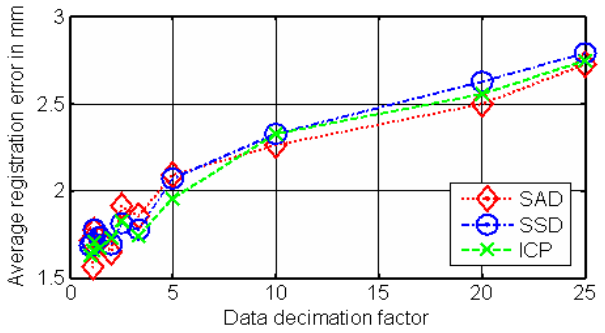

Figure 9: Decimation of the MRI head surface point set increases the registration error.

It is evident from Figure 9 that the smallest registration errors occur when undecimated head surface point sets with high spatial resolution are used, however the longest processing times are needed due to the large amount of data (see Figure 10). It was found that the ICP method has a processing time advantage, most clearly pronounced at high spatial MRI point set resolutions (it is the Nelder-Mead simplex method used for SAD and SSD that performs very slowly).

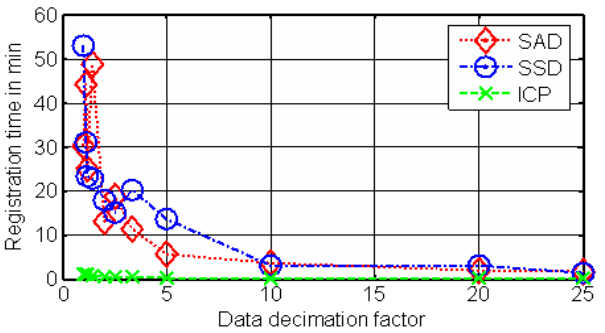

Figure 10: Decimation of the head surface point set decreases the registration time (shown for a Pentium IV with 1.7 GHz clock frequency).

ISSN: 1727-1983

Conclusions

3D surface-based registration can be realized in various ways. In this paper, we investigated the performance of three different surface-based methods to register two 3D point sets originating from MRI head scans and an electromagnetic tracking system providing the locations of EEG electrodes attached to the head. Basic image processing steps were performed to extract the head surface area from the digital 3D MRI data. To avoid gross misregistration due to the existing rotational symmetries of the point sets, a pre-registration method mainly building upon the singular value decomposition was implemented.

Pre-registered data were then fed into the SAD, SSD and ICP algorithms for final registration where, for the first two, the Nelder-Mead simplex method was used to minimize the registration error and find the corresponding 6 parameters of the rigid coordinate transformation that best matched the EEG with the MRI point set.

Our results show that registration errors down to about ≈1.55 mm per electrode can be achieved at the cost of longer processing times when MRI data with high spatial resolution (1 mm in each direction) are used. Furthermore, it was revealed that average surface point distances in the two point sets as high as 1-2 mm can occur in practice, mainly due to the difficulties in the proper mechanical positioning of the EEG electrodes when using an EEG cap.

We also investigated the effects of MRI data decimation on the registration performance. For example, when data decimation by a factor of 5 is applied, the average registration error increases by about 20% while the processing times decrease by factors of approximately 9 (SAD), 4 (SSD), and 5 (ICP).

All evaluated registration algorithms have sufficient registration performance for combined qEEG/MRI analysis and source localization methods, with the ICP method exhibiting the shortest processing time for the point sets used in this paper.

Acknowledgements

The authors would like to thank Mr. M. Deutschmann for helping with the MATLAB implementation of the ICP algorithm.

References

[1] TARANTOLA A. (1987): 'Inverse Problem Theory', (Elsevier, The Netherlands)

[2] PASCUAL-MARQUI R.D (1999): 'Review of methods for solving the EEG inverse problem', *Int. J. Bioelectromagn.*, **1** (1), pp. 75-86

[3] SREBRO R. (1996): 'An iterative approach to the solution of the inverse problem', *Electroencephalogr. Clin. Neurophysiol.*, **98**, pp. 349-362

[4] BAILLET S., GARNERO L. (1997) : 'A Bayeasian approach to introducing anatomo-functional priors in the EEG/MEG inverse problem', *IEEE Trans. Biomed. Eng.*, 44, pp. 374-385

[5] CLARKE C.J.S. (1994): 'Error estimates in the biomagnetic inverse problem', *Inverse Probl,.* **10**, pp. 77- 86.

[6] BOSCH-BAYARD J., VALDES-SOSA P., VIRUES-ALBA T., AUBERT-VAZQUEZ E., JOHN E.R., HARMONY T., RIERA-DIAZ J., TRUJILLO-BARRETO N. (2001), '3D statistical parametric mapping of EEG source spectra by means of variable resolution electromagnetic tomography', *Clin. Electroenceph.*, **32**, pp. 47-61

[7] FERNANDEZ-BOUZAS A., HARMONY T., FERNANDEZ T., SILVA-PEREYRA J., VALDES P., BOSCH J., AUBERT E., CASIAN G., OTERO OJEDA G., RICARDO J., HERNANDEZ-BALLESTEROS A., SANTIAGO E. (2000), 'Sources of abnormal EEG activity in brain infarctions', *Clin Electroencephalogr.*, **31**(4), pp. 165-169

[8] POLHEMUS INCORPORATED (2002): '3SPACE FASTRAK USER'S MANUAL'

[9] LITVIN F.L., FUENTES A. (2004): 'Gear Geometry and Applied Theory', (Cambridge University Press)

[10] SOILLE P. (2003): 'Morphological Image Analysis', (Springer, Berlin)

[11] GONZALEZ R.C., WOODS R.E., 'Digital Image Processing', (Addison-Wesley, New York)

[12] DHAWAN A. (2003): 'Medical Image Analysis', (Wiley-IEEE Press)

[13] HAJNAL J.V., HILL D.L.G, HAWKES D.J. (2001): 'Medical Image Registration', (CRC press)

[14] PELIZZARI C.A., CHEN G.T.Y., SPELBRING D.R. WEICHSELBAUM R.R., CHEN C.T. (1989): 'Accurate three-dimensional registration of CT, PET, and/or MR images of brain', *J. Comput. Assist. Tomogr.*, **13**, pp. 20-26

[15] LEVIN D.N., PELIZZARI C.A., CHEN G.T.Y., CHEN C.T., COOPER M.D. (1988): 'Retrospective geometric correlation of MR, CT, and PET images', *Radiology*, **169**, pp. 817-823

[16] LAGARIAS J.C., REEDS J.A., WRIGHT M.H., WRIGHT P.E. (1999): 'Convergence Properties of the Nelder-Mead Simplex Method in Low Dimensions', *MathSciNet SIAM J. Optim.,* **9** (1), pp. 112-147

[17] BESL P.J., MCKAY N.D. (1992): 'A method for registration of 3-D shapes', *IEEE Trans. Pattern Analysis and Machine Intelligence*, **14**(2) pp. 239-256

[18] HORN B.K.P. (1987): 'Closed-form solution of absolute orientation using unit quaternions', *Journal of the Optical Society of America A*, **4**, pp. 629-42

[19] DHAWAN A.P., ARATA L.K., LEVY A.V., MENTIL J. (1995): 'Iterative Principal Axes registration method for analysis of MR-PET brain images', *IEEE Trans. Biomed. Engineering*, **42**(11), pp. 1079-1087

[20] STRANG G. (1998), 'Introduction to Linear Algebra', (Wellesley-Cambridge Press, Cambridge)

ISSN: 1727-1983